Tools for the computation of acoustic parameters of narrow band high frequency clicks of odontocetes

Franck Malige[1,2], Margherita Silvestri[3], Mauricio Soto Gamboa[3], Iván A. Hinojosa[4,5,6,7], Gisela Giardino[8,9,2], Pascale Giraudet[1,2], Hervé Glotin[1,2], Ricardo Pereira[3], Angel Aguilar[3], Victor Molina[4], Fernanda Sotomayor[4], Agustina Macchi[8,9], Ignacio Rabinovich[8,9], Diego H. Rodriguez[8,9], Elisa Montti[10], Camille Nôus[11], and Julie Patris[1,2]

https://doi.org/to~be~precised

Abstract

Acoustic recording can be a very interesting way of monitoring cetaceans for conservation purposes. However, some sympatric species produce very similar sounds and are thus difficult to study specifically. In this work, we are interested in characterizing the narrow band high frequency (NBHF) clicks emitted by several species of odontocetes, among which all porpoises and some species of dolphins. The traditional acoustic parameters (durations, frequencies, bandwidths) of NBHF clicks show several drawbacks, such as redundancy, lack of precise definition, and poor robustness to noise. In this study, we propose a new method of characterizing NBHF clicks by fitting a Gabor wavelet to the signal and thus extracting two specific metrics, the Gabor frequency and the Gabor duration. We first assess the theoretical usefulness of this mathematical model, and then test it against traditional measurements in numerical examples with varying levels of noise. Our method is then applied to two empirical datasets recorded in South America, a place were many sympatric species are found to emit NBHF clicks. Two large sets of signals of Peale's dolphins (*Cephalorhynchus australis*) from Chaihuin bay, Chile on one hand, and Franciscana dolphins (*Pontoporia blainvillei*) from San Clemente del Tuyu, Argentina on the other hand, are thus analysed and compared. Our metrics allow a good characterization of each species' clicks in quick and efficient computation, with good reproducibility across different recording devices, and a clear separation of the two species. We suggest it could be applied to more datasets from different species, and possibly be used to classify NBHF of sympatric species.

Keywords: Odontocetes, acoustics, clicks

[1]DYNI team, LIS laboratory (CMR 7020), Aix-Marseille and Toulon university, France, [2]CIAN, international center of artificial intelligence in natural acoustics, France, [3]Universidad Austral de Chile (UACh), Chile, [4]Facultad de ciencias, departamiento de Ecología, Universidad Católica de la Santísima Concepción (UCSC), Concepción, Chile, [5]Center for Ecology and Sustainable Management of Oceanic Islands, Departamento de Biología Marina, Universidad Católica del Norte, (ESMOI),Coquimbo, Chile, [6]Centro de Investigación en Biodiversidad y Ambientes Sustentables, Universidad Católica de la Santísima Concepción, (CIBAS),Concepci ón, Chile, [7]Centro de Investigación Oceanográfica, Universidad de Concepción, (COPAS AUSTRAL), Concepción, Chile, [8]Universidad de Mar del Plata, Argentina, [9]Instituto de investigaciones marinas y costeras (IIMyC), FCEyN, UNMdP-CONICET, 7600, Mar del Plata, Argentina, [10]Vuelve al Oceano NGO, [11]https://www.cogitamus.fr/manifesteen.html

Correspondence
julie.patris@univ-amu.fr

Introduction

Coastal NBHF (Narrow Band High Frequency) odontocetes are resident species which are potentially threatened by human activities such as fishing, harbor development or fish farms (Jaramillo Legorreta et al., 2019; Silva et al., 2020). In this conservation context, it is very important to estimate which species are present in a specific zone or habitat, through long term monitoring (Amundin et al., 2022; Jaramillo Legorreta et al., 2019). However, visual monitoring of small cetaceans is costly and sometimes very difficult to implement in remote areas. As these species emit echolocation sounds most of the time (Andriolo et al., 2014), long term passive acoustic monitoring (PAM) is a good alternative to answer long term presence and density issues (Kimura et al., 2010; Marques et al., 2013; Soldevilla et al., 2008, 2010). When only one species is present in one site, unique data has been achieved in various instances through PAM (Amundin et al., 2022; Jaramillo Legorreta et al., 2019; Paitach et al., 2023). However sympatric species are also common in various zones (Kamminga et al., 1993; Kyhn et al., 2013). The context of the Southern Cone of Latin America is special since up to three from six NBHF species can share the same habitat (Acevedo, 2011; Heinrich et al., 2019; Hucke-Gaete et al., 2024; Malige et al., 2024; Morgenthaler et al., 2014). It is thus very important to be able to acoustically discriminate these species to assure the presence or measure the density of one particular species.

To acoustically describe the sound emitted by small cetaceans, a few classic indicators are usually used in bioacoustics. Since (Au, 1993), there has been a relative standardization of the measurements, mainly concerning frequency and duration parameters. This standardization allows reproducibility and the declared aim is often to find a way to differentiate species (Amorim et al., 2022; Reyes Reyes et al., 2018). For odontocetes species emitting narrow band high frequency echolocation clicks, however, this classification is difficult due to the high similarity of the clicks between species (see for example the comparison of NBHF clicks species from the South cone of America reported in Malige et al., 2025; Reyes Reyes et al., 2018). The classical NBHF clicks usually have a dominant frequency around 125-130 kHz, -10 dB duration around 50-100 μs, -3 dB bandwidth around 10 kHz and $Q_{-3\,\mathrm{dB}}$ value around 10-15 (Kamminga et al., 1996; Kyhn et al., 2009; Morisaka et al., 2011; Reyes Reyes et al., 2018). The differences in the averages of parameters coming from two species or two places (for the same species) is often of the order of the standard deviation of the series of values (Reyes Reyes et al., 2018). In the study by Kyhn et al., 2013, for example, clicks from two species of porpoises across two geographic regions are compared. In British Columbia, Canada, they recorded sympatric harbor porpoise (*Phocoena phocoena*) and Dall's porpoise (*Phocoenoides dalli*) while in Denmark, they recorded harbor porpoise, the only porpoise species present in that region. They found that "*Danish harbour porpoise clicks were more similar to Dall's porpoise than to their conspecifics in Canada*". Captive Yangtze finless porpoises (*Neophocaena asiaeorientalis*) and dwarf sperm whales (*Kogia sima*) produce NBHF clicks which parameters are statistically different from their free-ranging conspecifics (Fang et al., 2015; Malinka et al., 2021). Franciscana dolphins (*Pontoporia blainvillei*), another exclusive NBHF species, showed a different source of acoustic variation : neonates produce broader bandwidths and greater parameter dispersion (Giardino et al., 2024; Melcon et al., 2016) adding more complexity to the challenge of classification. Some NBHF species, such as the members of the Cephalorhynchus genus, emit other types of clicks, along with the typical NBHF click (Martin et

al., 2019, 2018, 2021; Martin et al., 2024; Nielsen et al., 2024), which could be useful to differentiate species. However, this behavior is not systematically observed (Malige et al., 2025) and has been little studied to date. Thus, precise acoustic description of the classical NBHF echolocation clicks is very important for numerous studies. To our knowledge, except the pioneer work of C. Kamminga (Kamminga et al., 1996, 1993) no other method than the statistical study of the classical acoustic parameters has been proposed to date to discriminate between NBHF species and the results are still disappointing and lack reproducibility (Reyes Reyes et al., 2018).

Along with the high similitude between species, the classical acoustic parameters used to date show several problems. The first one is that the duration and frequency of a click are not easily defined. Clicks are transient signals for which frequency is difficult to define precisely. Usually, at least two distinct measures of the "frequency" content of a click are used : the peak frequency and the centroid frequency (Au, 1993). As we show in this work, both have several drawbacks, and can be seriously affected by noise, by the choice of the recording device parameters (set up, position), or by post-recording processing (filtering). Similarly, the definition and measurement of the duration of a click is not trivial. It is usually estimated by means of the computation of its envelope and can be highly dependent on the SNR (signal to noise ratio). What's more, many clicks present replicas of the first oscillations (sometimes difficult to separate from the first signal), thus increasing the duration of the click. A clarification and quantitative study of the estimation of the usual parameters of a NBHF click seems a prerequisite to achieve a successful classification based on acoustic detections (Song et al., 2017; Zimmer, 2011). In this paper, we describe in detail the drawbacks which appear when using the classical acoustic parameters to classify NBHF clicks. Then, by means of numerical tests on synthesized clicks (Gabor wavelets, Gabor, 1946), we present the influence of noise, distortion and replicas over the potential bias and the precision of the measurements.

In our study, the Gabor wavelets are also used as a theoretical tool to better understand the link between several classical parameters and to show their possible redundancy, as well as a practical tool to measure these parameters (by the fitting of this mathematical function to the signal as was proposed several decades ago by (Kamminga et al., 1996; Wiersma, 1982) (see also Lelandais and Glotin, 2008; Madhusudhana et al., 2015; Trone et al., 2015). The methods developed in this paper are finally applied to two data sets, recorded with two different devices in two different places. The first data set was obtained in Chaihuin, región de los Rios, Chile, in September 2023 where a group of Peale's dolphins (*Cephalorhynchus australis*) is present (Galatius et al., 2025; Malige et al., 2024). The second data set was obtained near San Clemente del Tuyu, in Samborombón bay, región de Buenos Aires, Argentina, in September 2025 with presence of Franciscanas (*Pontoporia blainvillei*) (Bastida et al., 2022; Wells et al., 2021). Analyzing these two data sets, we were able to compare the results of the different methods (classical parameters, fitting of a Gabor wavelet) to discriminate between NBHF species.

1. Materials and methods

In this section, we first present the data sets collected in the field works. Secondly, we present the parameters used to characterize the NBHF clicks and several problems in their estimation. Then, a presentation of the Gabor wavelet mathematical function and the analytical computation of its acoustic parameters is done and, using this function, we analyze the possible effects of replicas on the measurements of the parameters. Finally we present the numerical tests, which

aim to provide values of the bias and precision on the parameters estimation, and the statistical analysis done afterwards.

1.1. Data set and click detections

We collected visual and acoustic data during 3 days in September 2023 in Chaihuin bay, Región de los rios, in Chile, in a zone where Peale's dolphins (*Cephalorhynchus australis*) were known to be present. The duration of the recordings was 75 hours, from the 21st to the 24th of September 2023. Two devices were installed at latitude $39^o57'16.9''S$ and longitude $73^o36'14.5''W$ in a sandy 17 m depth zone, around 100 m from the shore, at the South entrance of the bay :

- the recording system HighBlue (Barchasz et al., 2020) along with two hydrophones (C57, channel 1, and C55, channel 2, from Cetacean Research, *http://cetaceanresearch.com/*). The distance between the two hydrophones is 60 cm. C55 and C57 have a cylindrical transducer (omni-directional until 10 kHz, sensitive in the mid-plane for high frequencies). Their frequency sensitivity is linear within -12 dB from 8 Hz to 100 kHz (manufacturer's documentation). We checked that the acquisition chain has a flat response in frequency up to over 150 kHz, based on our subsequent calibrations, realized in the LMA laboratory of Aix-Marseilles university. A more complete description of the recording device is given in (Patris et al., 2023). The set up chosen was a dynamic of 16 bits, a sampling frequency of 512 kHz, a duty cycle of 9 min IN/ 1 min OFF, two channels. The device was installed on the sea floor (as in Malige et al., 2025; Patris et al., 2023), 17 m below the surface.
- a Soundtrap model 600 HF was also installed, at a horizontal distance of 1 m to the HighBlue device, 10 m below the surface and 7 m above the sea floor, in a moored line with a submerged buoy. The set up chosen was a dynamics of 16 bits, a sampling frequency of 384 kHz, continuous recording, one channel. Files of 10 min durations were obtained.

We collected visual and acoustic data during 6 days in September 2025 near San Clemente del Tuyu, in Samborombón bay, provincia de Buenos Aires, in Argentina, in a zone where Franciscanas (*Pontoporia blainvillei*) were known to be present. The duration of the recordings was 120 hours, from the 10th to the 15th of September 2025. Three devices were installed at latitude $36^o15'00.0''S$ and longitude $56^o52'05.0''W$ in a 2-4 m depth zone (depending on the tide), around 9 km from the shore (Punta Rasa, San Clemente del Tuyu) :

- the recording system HighBlue along with two C57 hydrophones. The set up chosen was a dynamics of 24 bits, a sampling frequency of 512 kHz, continuous recording. The device was installed on an iron structure on the sea floor, at a mean depth of 3 m. Files of 5-min duration were obtained.
- a Soundrap model ST300HF was also installed in the iron structure, at 40 cm to the channel 2 of the HighBlue device. The set up chosen was a dynamics of 16 bits, a sampling frequency of 576 kHz, continuous recording, one channel. Files of 10 min durations were obtained.
- a FPOD (a commercial click detector developed by Chelonia Limited, Tregenza, 2014), was also installed in the iron structure at 47 cm from the channel 1 of the HighBlue. The F-POD works in the 20 kHz - 160 kHz range, detects and logs all potential clicks in this frequency range, registering several parameters for each detection (central frequency, duration, etc.) as well as the ambient sea water temperature and its vertical angle.

For the San Clemente data set, we used the FPOD detections (achieved with the dedicated software from Chelonia) to select wav files from the two other devices. These detections are usually reliable to indicate periods when odontocetes are present (Malige et al., 2025; Patris et al., 2023). The click detection in the two data sets was then achieved as presented in (Patris et al., 2023) in all the wav files of the Chaihuin data set and in the selected wav files for San

Clemente. The click detector, written in OCTAVE (Eaton et al., 2009), is based on a three step procedure. First, all files are high pass filtered (100 kHz). Second, a first level of detection is selected when the amplitude of the filtered signal is above a chosen threshold (V_1) multiplied by the whole energy of the filtered signal of the file. Finally, for each first detection, a FFT (fast Fourier transform) of 1 ms (512 pts) of the signal (without filtering) is performed. Then we measure the energy of the obtained spectrum in the frequency band of 120-140 kHz ($E_{120-140}$), and discard the detections that have high energy in the 30-90 kHz bandwidth (E_{30-90}). These signals are usually broadband signals considered as noise : knocks on the devices (from sand grain for example) or shrimps clicks (Verluis et al., 2000). In practice, we compared $E_{120-140}$ to $V_2 \times E_{30-90}$ where V_2 is another adaptable threshold. Details for each data set and each device are presented in supplementary materials. The aim of our study is to measure the acoustic parameters of the high SNR NBHF clicks from Peale's dolphins and Franciscanas recorded by distinct instruments. Thus, we chose to have a true positive rate higher than 95%, regardless of the false negative rate. As clicks usually come in groups, we discarded files containing less than 20 detections for parameters estimation, to further reduce the number of false positives, also at the risk of missing a few individual clicks. Finally, a manual revision of all detections was achieved for all the selected files to remove eventual false positives such as artificial sonars, broadband signals or cluttering. The signal to noise ratio (SNR) was computed for each detection as $SNR = 10 \times log(\frac{E_{signal}}{E_{noise}})$ where E_{signal} is the variance of the signal during 0.1 ms centered on the click, while E_{noise} is the variance of a portion 0.1 ms of the sound, centered at 0.3 ms before the detection.

1.2. Parameters of odontocetes clicks

1.2.1. Classical parameters. The classical acoustical parameters used in marine bioacoustic (Au, 1993) and in studies of NBHF clicks are : the mean date of the signal t_c, the duration of the signal at -10 dB ($\Delta t_{-10\,\mathrm{dB}}$) and at -20 dB ($\Delta t_{-20\,\mathrm{dB}}$), the 'rms' duration ($\Delta t_{\mathrm{rms}}$ for 'root mean square'), the 'peak' frequency f_p of the signal, the 'centroid' frequency f_c, the bandwidths at -10 dB and -3 dB ($\Delta f_{-10\,\mathrm{dB}}$ and $\Delta f_{-3\,\mathrm{dB}}$), the characteristic bandwidth 'rms' (Δf_{rms}) and the factor of quality at -3 dB ($Q_{-3\,\mathrm{dB}}$). The definitions of the parameters associated with a signal $s(t)$ (and its Fourier transform, defined by the formula $S(f) = \int_{-\infty}^{+\infty} s(t)e^{-2i\pi ft}dt$) are :

- The energy of the signal $E = \int_{-\infty}^{+\infty} |s(t)|^2 dt \; = \int_{-\infty}^{+\infty} |S(f)|^2 df$
- The mean date of the signal defined by $t_c = \frac{\int_{-\infty}^{+\infty} t|s(t)|^2 dt}{\int_{-\infty}^{+\infty} |s(t)|^2 dt}$.
- The duration 'rms' : $\Delta t_{\mathrm{rms}} = \sqrt{\frac{\int_{-\infty}^{+\infty} (t-t_c)^2 |s(t)|^2 dt}{\int_{-\infty}^{+\infty} |s(t)|^2 dt}}$.
- The duration at -10dB (Δt_{-10dB}) is defined as the duration when the envelope of the signal is above the maximum of the envelope divided by $\sqrt{10}$. In practice, we get the envelope taking the modulus of the Hilbert transform of the signal.
- The duration at -20dB (Δt_{-20dB}) is defined as the duration when the envelope of the signal is above the maximum of the envelope divided by 10
- The peak frequency f_p is the frequency where the modulus of the spectrum $|S(f)|$ of the signal is maximum.
- The 'centroïd' frequency f_c is defined by the formula $f_c = \frac{\int_{-\infty}^{+\infty} f|S(f)|^2 df}{\int_{-\infty}^{+\infty} |S(f)|^2 df}$.
- The 'rms' bandwidth : $\Delta f_{\mathrm{rms}} = \sqrt{\frac{\int_{-\infty}^{+\infty} (f-f_c)^2 |S(f)|^2 df}{\int_{-\infty}^{+\infty} |S(f)|^2 df}}$

- The bandwidth at -3dB (Δf_{-3dB}) is the length of the interval around f_p where the modulus of the spectrum is larger than $\frac{max(|S(f)|)}{\sqrt{2}}$
- The bandwidth at -10dB (Δf_{-10dB}) is the length of the interval around f_p where the modulus of the spectrum is larger $\frac{max(|S(f)|)}{\sqrt{10}}$.
- The quality factor at -3dB is $Q_{-3dB} = \frac{f_c}{\Delta f_{-3dB}}$.
- The quality factor 'rms' is $Q_{rms} = \frac{f_c}{\Delta f_{\text{rms}}}$.
- The duration-bandwidth product 'rms' is $\Delta t_{\text{rms}} \times \Delta f_{\text{rms}}$

All these classical parameters were computed for each click detection in our data set, as presented in (Patris et al., 2023).

1.2.2. *Issues with classical parameters.*

- The centroid frequency is confusedly defined in Au, 1993 : considering the normalized energy of the spectrum as a density probability of the random variable f, it is defined as the *mean* of the frequency (eq (10-1), page 217, in Au, 1993) or the *median* of the frequency (the frequency dividing the spectra in two parts of equal energy, in the paragraph following eq (10-1)). The reference Au, 1993 is given for the computation of centroid frequency in most papers dealing with NBHF clicks species, some authors use a definition, others use the other one, and most don't specify.
- The peak frequency distribution of measured NBHF clicks are plurimodal (several local maxima in the distribution) in various studies, such as (Kamminga et al., 1986; Malige et al., 2025; Malinka et al., 2021; Merkens et al., 2018; Morisaka et al., 2011; Patris et al., 2023; Reyes Reyes et al., 2015). This comportment of the peak frequency is in contrast with the comportment of the centroid frequency which has usually only one mode. Thus the plurimodal distribution of peak frequency may not reflect a diversity of clicks' production but rather be a consequence of propagation (see section 1.3.4).
- Signals recorded in the field often have one or more replicas and these replicas can have a significant influence on the calculation of the parameters and therefore their accuracy (Li et al., 2005) and section 1.3.4.
- The robustness of these parameters to the usual sources of noise has not been quantified, thus the parameters may be differently affected in different experiments.

1.3. Use of Gabor wavelets

1.3.1. *Definition.*

In an attempt to improve the classification and clarify the importance of each parameter in this classification, we studied the adjustment of a mathematical function to these signals. Indeed, NBHF clicks from various species, including Franciscanas and Peale's dolphins (presented in figure 1, left), highly resemble a Gabor wavelet, as can be seen in figure 1 (right) and in (Au et al., 1999; Kamminga et al., 1996, 1993; Macaulay et al., 2020).

Gabor wavelets are given by the formula:

$$g(t) = A\, e^{-\frac{(t-t_0)^2}{\tau^2}}\, cos(2\pi f_0(t-t_0)+\phi) \quad (1)$$

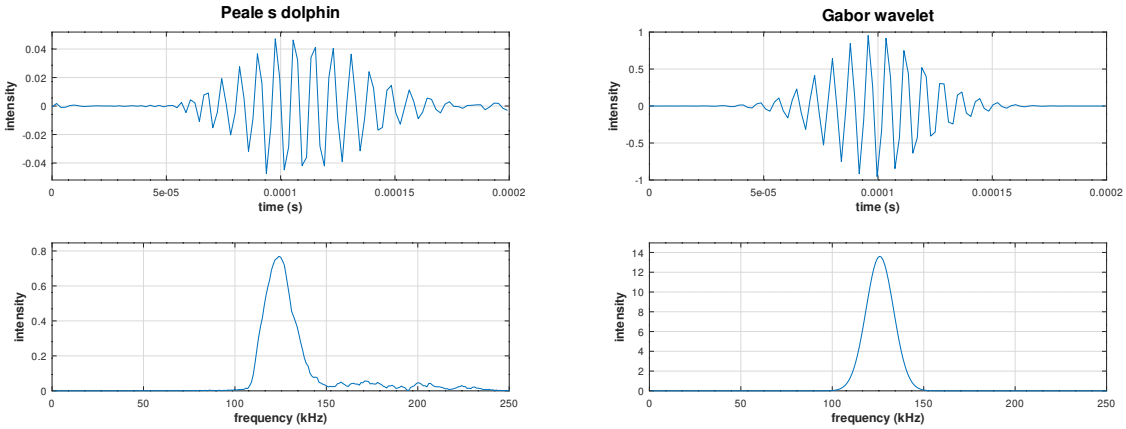

Figure 1 – *Left : waveform (above) et spectrum (below) of a typical click from a Peale's dolphin (Cephalorhynchus australis) recorded in Chaihuin, sept 2023 - sampling frequency of 512 kHz. Right : a Gabor wavelet (waveform and spectrum), with $A = 1$, $t_0 = 0.0001$ s, $f_0 = 125$ kHz, $T = 30$ μs and $\phi = 0$ and a sampling frequency of 512 kHz (see formula 1).*

This set of mathematical functions is defined by 5 independent parameters (A, t_0, T, f_0 and ϕ) : a Gaussian, of amplitude A, centered at t_0, and with a standard deviation $\sigma = \frac{T}{\sqrt{2}}$ multiplies a cosine function of frequency f_0 and phase shift ϕ at $t = t_0$. The Gaussian $A\, e^{-\frac{(t-t_0)^2}{T^2}}$ is the envelope of the signal. One of the most important traits of NBHF clicks is that they are narrowband signals, which is related to the fact that we "see" a lot of oscillations in the signal (Zimmer, 2011). This is the case when the Gabor wavelet has $f_0 > \frac{1}{T}$ or, equivalently $T > T_0$ where $T_0 = \frac{1}{f_0}$ corresponds to the period of the cosine. These signals have been named *polycyclic* (we see several oscillations) in opposition to *oligocyclic* signals, such as bottlenose dolphin's or sperm whale's clicks, for example, which usually have less than four visible oscillations (Goold and Jones, 1995; Kamminga et al., 1996) and are broadband signals. The use of Gabor wavelet has three advantages. First, we can use them as a good model to compare to odontocete signals (figure 1). The second advantage is that for these functions, the analytical computation of the classical acoustic parameters is quite simple, as we will see in the following section. The third advantage is that we can also easily compute these parameters in the presence of a replica (see section 1.3.4).

1.3.2. Classical parameters for a Gabor wavelet . Table 1 gives the classical parameters computed for a Gabor wavelet (proofs are given in the supplementary materials). The typical and conservative values for NBHF clicks of $f_0 \simeq 100$ kHz and $T \simeq 20\mu$s leads to $f_0 \times T \simeq 2$. For these values, the classical factor $e^{-\pi^2 T^2 f_0^2}$ present in various results (see supplementary materials) is close to 10^{-17} and can be considered equal to zero (*polycyclic* approximation).

In the *polycyclic* approximation, the peak frequency f_p is equal to f_0 (see table 1). Due to the symmetry of the spectrum with respect to zero (see proofs in the supplementary materials), the centroid frequency f_c of a Gabor wavelet is zero. Nevertheless, in practice, if we compute f_c using only positive values of f in the spectrum, then $f_c = f_0$. The parameters f_p and f_c are therefore good estimators of the parameter f_0 of this signal, without bias. They are strongly redundant when estimating the frequency of a signal having the shape of a Gabor wavelet. In table 1, we can also see that durations and bandwidths depend only on the parameter T. Thus, these classical parameters are strongly redundant to classify signals with the characteristics of a Gabor wavelet. The quality factor at -3 dB is $\frac{\pi}{\sqrt{2ln(2)}} f_0 T$ and the 'rms' quality factor is $2\pi f_0 T$. These two quality

Table 1 – List of computed parameters for Gabor wavelets (formula 1) in the polycyclic approximation ($e^{-\pi^2 T^2 f_0^2} \to 0$)

Parameters	symbol	Gabor wavelet
Signal	$g(t)$	$Ae^{-\frac{(t-t_0)^2}{T^2}}\ cos(2\pi f_0(t-t_0)+\phi)$
Fourier transform	$G(f)$	$\frac{\sqrt{\pi}AT}{2}[e^{-\pi^2T^2(f-f_0)^2}e^{i\phi}$ $+e^{-\pi^2T^2(f+f_0)^2}e^{-i\phi}]e^{-2i\pi ft_0}$
Energy	E	$\sqrt{\frac{\pi}{2}}A^2T$
Average date	t_c	t_0
Duration at -10dB	$\Delta t_{-10\text{dB}}$	$\sqrt{2ln(10)}\ T \simeq 2.15\ T$
Duration at -20dB	$\Delta t_{-20\text{dB}}$	$\sqrt{4ln(10)}\ T \simeq 3.03\ T$
Duration 'rms'	Δt_{rms}	$\frac{1}{2}\ T$
Peak frequency	f_p	f_0
Centroid frequency	f_c	0 (or f_0 if we consider only positive frequencies)
Bandwidth at -3dB	$\Delta f_{-3\text{dB}}$	$\frac{\sqrt{2ln(2)}}{\pi}\ \frac{1}{T} \simeq 0.37\ \frac{1}{T}$
Bandwidth at -10dB	$\Delta f_{-10\text{dB}}$	$\frac{\sqrt{2ln(10)}}{\pi}\ \frac{1}{T} \simeq 0.68\ \frac{1}{T}$
Bandwidth 'rms'	Δf_{rms}	$\frac{1}{2\pi}\ \frac{1}{T} \simeq 0.16\ \frac{1}{T}$
Quality factor at -3dB	$Q_{-3\text{dB}}$	$\frac{\pi}{\sqrt{2ln(2)}}\ f_0 T \simeq 2.67\ f_0 T$
Quality factor 'rms'	Q_{rms}	$2\pi f_0 T \simeq 6.28\ f_0 T$
'rms' duration-bandwidth product	P_{incert}	$\frac{1}{4\pi}$

factors are proportional to the product $f_0 T = \frac{T}{T_0}$ and are therefore proportional to the number of oscillations that we "see" in the signal. Finally, for a Gabor wavelet, the duration-bandwidth product 'rms', $\Delta t \times \Delta f$ is always equal to $\frac{1}{4\pi}$ (in the *polycyclic* approximation). It has been proven that any other signal has a duration-bandwidth product 'rms' larger than $\frac{1}{4\pi}$ (Gabor, 1946) which proves that Gabor wavelet presents a good compromise between time and frequency precision.

1.3.3. Fitting. For each click detection, we fitted a Gabor function to the waveform of the click (after a high pass filter at 100 kHz), by means of the function *leasqr* in Octave. The estimation of f_0 is called Gabor frequency of the click (f_{Gabor}), the estimation of T is called Gabor duration of the

click (T_{Gabor}) and $\frac{1}{T}$ is called Gabor bandwidth of a click (Δf_{Gabor}). We set the initial parameters of the fitting as : A_{init} is the maximum value of the waveform of the detected click, $t_{0,\text{init}}$ is the date of the maximum of the waveform (we fitted the Gabor wavelet only on 50 μs of the signal, centered on this value), T_{init} is 50 μs, $f_{0,\text{init}}$ is the peak frequency of the click (previously computed, see section 1.2.1), ϕ a uniformly random angle between 0 and 2π. We oversampled the signal by a factor 4 (function *interp* in Octave), because the convergence of the OCTAVE function *leasqr* was easier. For analysis, we selected only clicks for which the fitting of a Gabor wavelet converged as given by the *leasqr* function in OCTAVE.

1.3.4. Replicas . Another difficulty for the measurement of the parameters is the presence of signal's replica in NBHF clicks (see figure 2 and comparison with figure 1, left), usually after a few tens of μs, for various species of dolphins and porpoises (Finfer et al., 2012; Kamminga et al., 1996; Kyhn et al., 2009; Merkens et al., 2018; Morisaka et al., 2011; Song et al., 2017; Tougaard and Kyhn, 2009; Villadsgaard et al., 2007).

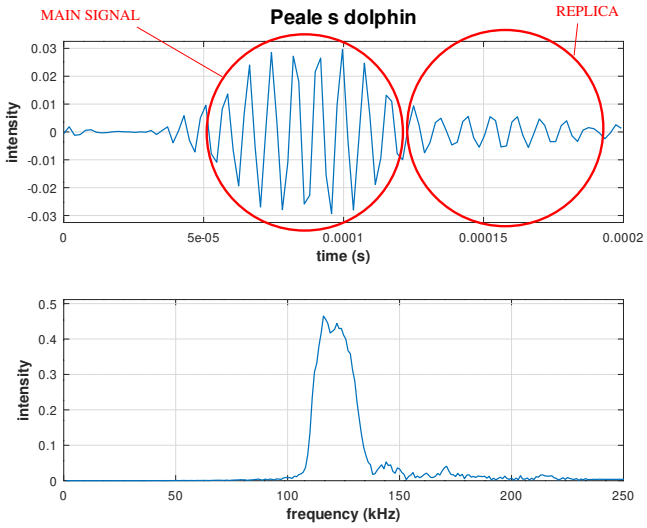

Figure 2 – *Waveform (above) et spectrum (below) of a typical click from a Peale's dolphin with a replica, recorded in Chaihuin, sept 2023 - sampling frequency of 512 kHz.*

These replicas can have three origins. First, dolphins or porpoises could emit a signal composed of various similar signals. Secondly, replicas could come from internal reflexions in the body of the animal : the fact that the signal is strongly attenuated and distorted when off axis (Macaulay et al., 2020) indicates the influence of internal processes. Finally, replicas could come from external reflections during propagation (in the surface of the sea, the ground or even the recording instrument). This last phenomenon of external reflections is particularly present in shallow waters where cluttering can be intense. In deeper waters, replicas are not so common (Malinka et al., 2021). In any case, we can approximate the signal containing a replica as $x(t) = g(t) + a\, g(t-\tau)$ where τ is the time delay of the replica, a is a real coefficient representing the attenuation of the main signal and g is a Gabor wavelet. The value of a is usually between -1 and 1 but in some case can have a modulus greater than 1 (Song et al., 2017). In the following sections we examine the effect of the replica on the classical parameters of the signal.

Effect of replicas on frequencies. As we demonstrated, for a simple signal without noise, peak frequency f_p and centroid frequency f_c are good estimators of the parameter f_0 of the Gabor wavelet. Nevertheless, in the presence of one or more replicas, the precision of the two estimators is strongly degraded. The Fourier transform of x is $X(f) = G(f) \times (1 + ae^{-2i\pi f\tau})$ where G is the Fourier transform of the Gabor wavelet g (see proof in the supplementary materials). The modulus of the coefficient $1 + ae^{-2i\pi f\tau}$ is a periodic function of f, with a period of $1/\tau$ and, therefore, in the spectrum, oscillations of period $1/\tau$ appear. An example of a synthesized click, composed of a Gabor wavelet and its replica, is given in figure 3. The replica arrives at $\tau = 200$ μs after the signal and produces an oscillation of the spectrum at $\frac{1}{\tau} = 5$ kHz. Another example can be seen when we compare figure 1 (left) where the peak is well defined in the spectrum and figure 2 where the position of the peak is not clear, due to the presence of the replica.

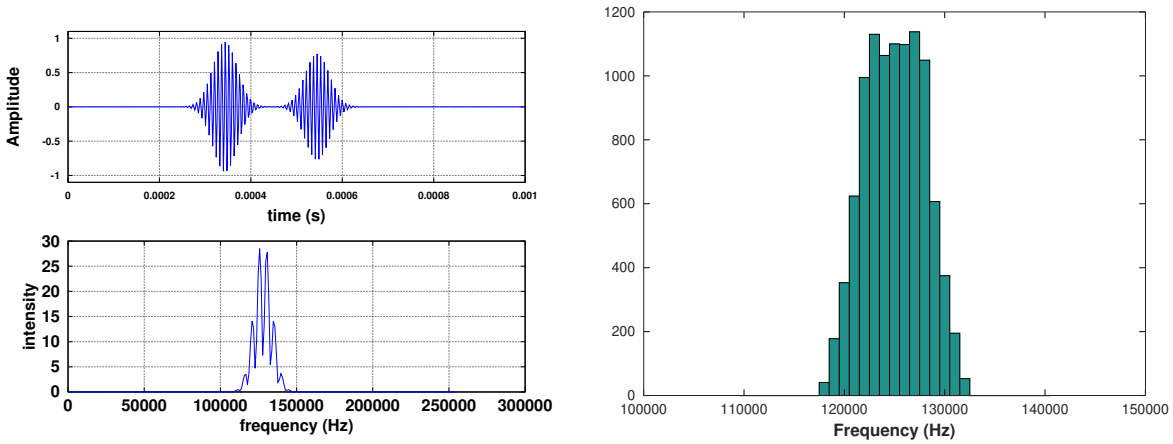

Figure 3 – *Left Top : Waveform of a signal composed of a Gabor wavelet (with parameters $A = 1$, $t_0 = 350\mu s$, $f_0 = 127kHz$, $T = 38.6\mu s$, $\phi = 3.248$) and a replica separated by $\tau = 200\mu s$ with an attenuation coefficient $a = 0.7$. Left Bottom : The spectrum is composed of the Gaussian centered at $f_0 = 127$ kHz and periodic variations which are superimposed, of period $\frac{1}{\tau}$ = 5 kHz. Right : Histogram of peak frequencies for 10000 theoretical clicks, composed of a gabor wavelet with one replica (parameters : $A = 1$, $f_0 = 125$ kHz, $t_0 = 0$, $T = 30$ μs, $\phi = 0$. The coefficient a follows a normal distribution with a mean of 0.8 and standard deviation of 0.2. The delay τ follows a uniform distribution in the interval [10 μs ; 150 μs].*

Therefore, in the case of a signal corresponding to figure 3 (left), due to the replica, it is difficult to measure accurately the peak frequency using the spectrum. Typically, we have an uncertainty of the order of $\frac{1}{\tau}$ for the estimation of the frequency peak (Song et al., 2017; Wiersma, 1982). In figure 3 (right), we present an histogram of the peak frequencies obtained for 10000 synthesized clicks composed of a Gabor wavelet (with $f_0 = 125$ kHz) and a replica, computed using the formulas presented above. The chosen values of τ follow a uniform distribution in the interval [10 μs ; 150 μs], which are common values for the delay in real clicks. We clearly see that the presence of replicas increase the uncertainty of the measure and that modes are present around 123 and 127 kHz. The average value of f_p is very close to 125 kHz but the standard deviation is quite high (around 3 kHz) when in the absence of replica the standard deviation of the measure is close to zero. Therefore, the presence of the replica strongly degrades the precision of the measure of f_p. Regarding the centroid frequency of a Gabor wavelet with replica, a similar phenomenon appears. It can be shown (see supplementary materials) that:

$$f_c = f_0 - \frac{\frac{a\tau}{\pi T^2} sin(2\pi f_0 \tau)) e^{-\frac{\tau^2}{2T^2}}}{1 + a^2 + 2a\ cos(2\pi f_0 \tau) e^{-\frac{\tau^2}{2T^2}}} \quad (2)$$

When a tends toward zero (faint replica) we found logically that f_c tends toward f_0. Conversely, when a is not close to zero, f_c and f_0 can differ a few kHz.

Effect of replicas on durations and bandwidths. The click duration logically increases when a replica is present. For example, the duration "rms" can be computed analytically in the case of a Gabor wavelet with a replica. The formula (proven in supplementary materials, for $t_0 = 0$) is :

$$\Delta t_{\text{rms}} = \sqrt{\frac{t_c^2 + \frac{T^2}{4} + \frac{a^2}{1+a^2}\tau(\tau - t_c) + \frac{2a}{1+a^2} t_c^2\ cos(2\pi f_0 \tau) e^{-\frac{\tau^2}{2T^2}}}{1 + \frac{2a}{1+a^2}\ cos(2\pi f_0 \tau) e^{-\frac{\tau^2}{2T^2}}}} \quad (3)$$

where

$$t_c \simeq \frac{a^2\tau + a\tau\ cos(2\pi f_0 \tau) e^{-\frac{\tau^2}{2T^2}}}{1 + a^2 + 2a\ cos(2\pi f_0 \tau) e^{-\frac{\tau^2}{2T^2}}} \quad (4)$$

This formula is not easily interpretable but shows that the duration of a signal with a replica increases in a complex way. In the case of the durations $\Delta t_{-10\text{dB}}$ or $\Delta t_{-20\text{dB}}$, commonly used in various studies, the presence of the replica changes also the value due to the change of the envelope of the signal, usually in a non obvious way. The different measures of bandwidths of a signal with a replica are also changed. For example, "rms" bandwidth is given by the formula :

$$(\Delta f_{\text{rms}})^2 = (f_0 - f_c)^2 + \frac{1}{4\pi^2 T^2} - a e^{-\frac{\tau^2}{2T^2}} \frac{cos(2\pi f_0 \tau)\frac{\tau^2}{\pi^3 T^4} + 4sin(2\pi f_0)(f_0 - f_c)\frac{\tau}{2\pi T^2}}{1 + a^2 + 2acos(2\pi f_0 \tau) e^{-\frac{\tau^2}{2T^2}}} \quad (5)$$

Conclusions. Globally, the presence of the replica degrades the precision of the measures of all acoustic parameters. We chose to fit only one Gabor wavelet to our signals, hoping that the fitting of one function on the main signal will reduce the influence of the replica in estimating the parameters. This hypothesis is tested numerically in the next section.

1.4. Numerical tests

The clicks of NBHF odontocetes are often quite similar between species and consequently, the parameters calculated are also similar. Even if the cited studies present statistical indicators of data dispersion, there is rarely a study of the error made in estimating these parameters. Dispersion may come from the diversity of the clicks emitted but also from the way of measuring the signals. This implies the need to assess estimators of the parameters in terms of potential bias and in terms of precision. In order to have a clearer view of the errors in estimating the acoustic parameters of the real signal, we performed these estimations in synthetic, known clicks : noisy Gabor wavelets.

Noisy Gabor wavelet. The computation of clicks acoustic parameters and the Gabor fitting have been tested on simulated clicks, using a dedicated OCTAVE program (available at *https://zenodo.org/*

records/18223438) in order to compare methods of estimation. We have generated noisy Gabor wavelets ($N = 40000$) of the form :

$$x(t) = A\, e^{-\frac{(t-t_0)^2}{T^2}}\, cos(2\pi f_0(t-t_0)+\phi) \quad + \quad n(t) \tag{6}$$

The chosen parameters were the following : the duration of the signal is 1 ms (t is taken in the interval [0;1ms]), $A = 0.8+0.4X_{[0;1]}$ where $X_{[0;1]}$ is the random variable of continuous uniform distribution on the interval $[0; 1]$. Similarly, the Gabor frequency is $f_0 = 125000\times(0.98+0.04X_{[0;1]})$ Hz, the average date of the wavelet is $t_0 = 450 + 100X_{[0;1]}$ (in micro seconds), the characteristic time of duration is $T = 20 + 60X_{[0;1]}$ (in micro seconds), phase shift $\phi = 2\pi X_{[0;1]}$ rad. We then added a Gaussian noise $n(t)$ to the signal for which the values follow a gaussian distribution $N(0;\sigma)$. The values of the standard deviation σ where taken from 0.001 to 0.4 (100 synthetic clicks for each value of σ) in order to have a uniform repartition of the SNR. The created function is then sampled at 512 kHz. For each signal the SNR was measured as presented in section 1.1.

Parameters estimation. We measured the acoustic parameters of the signal in various ways, which we compare with the exact value of the parameters of the Gabor wavelet, given in table 1. For each synthesized signal, the frequency f_0 was estimated by four methods, as presented in section 1.2 : the peak frequency of the spectrum, the centroid frequency, the number of sign changes of the waveform and the adjustment of a Gabor wavelet. Similarly, we measured the various values of the duration of a click (duration -10 dB, duration -20 dB, rms duration, adjustment by Gabor wavelet) and we compared it to the actual value depending on T of the Gabor wavelet using the table 1. We also measured the various values of the frequency band of a click ($\Delta f_{-3\text{dB}}$, $\Delta f_{-10\text{dB}}$, Δf_{rms}) and the corresponding value depending on T given in table 1. For all the measures of frequencies, durations and bandwidths, we estimated the *bias* (resp. *precision*) of the measures as the average (resp. standard deviation) of the percentage of the errors. Then we represented the bias and precision of each method, as a function of the SNR.

Other numerical tests. The same measurements were also conducted for two other types of signal :

- a "distorted" Gabor wavelet (the Gabor wavelet was multiplied by an affine function equal to 1 in t_0 and 0 when $t = t_0 - 2T$).

$$x(t) = A\, e^{-\frac{(t-t_0)^2}{T^2}}\, cos(2\pi f_0(t-t_0)+\phi) \times (1+\frac{t-t_0}{2T}) + n(t) \tag{7}$$

- a Gabor wavelet with replica :

$$x(t) = A\, e^{-\frac{(t-t_0)^2}{T^2}}\, cos(2\pi f_0(t-t_0)+\phi) + a\, A\, e^{-\frac{(t-t_0-\tau)^2}{T^2}}\, cos(2\pi f_0(t-t_0-\tau)+\phi) + n(t) \tag{8}$$

In the latter case, the delay τ and the attenuation a follow the following laws: $\tau = 20 + 80X_{[0;1]}$ (in μs) and $a = 0.1 + 0.5X_{[0;1]}$ (weak replica) or $a = 0.5 + 0.6X_{[0;1]}$ (strong replica).

1.5. Statistical analysis

We studied the statistical difference of the relevant acoustic parameters of the NBHF clicks from the two species (Peale's and Franciscana dolphins) of the two datasets. Mean and standard deviation of the acoustic parameters were calculated. Histograms of the acoustic parameters were plotted to visualize the statistical distribution of these parameters. When it was adequate a gaussian was fitted to the parameters histogram. A linear discriminant analysis (LDA) for the two datasets was conducted using values of f_{Gabor}, f_{peak}, T_{Gabor} and ΔT_{-10dB}. Prior probabilities were estimated from the observed proportion of confirmed detections of each dataset. These statistical analyses were conducted in R version 4.4.0 (R Foundation for Statistical Computing, 2024). Linear discriminant analysis (LDA) was performed using the MASS package (Venables and Ripley, 2002). We computed a non-parametric Wilcoxon rank-sum test (Mann–Whitney) for each relevant parameter between the two different data sets using Octave. Finally a test was proposed to estimate if the parameters from a randomly extracted subset of 10 clicks from San Clemente are compatible with the distribution of these parameters in the Chaihuin dataset (following Krzywinski and Altman, 2013).

2. Results and Discussion

2.1. Numerical tests

In this section, we present some of the results of the estimation of frequencies, durations and bandwidths of the synthesized clicks by different methods presented in section 1.4. All the results of the numerical tests are presented in supplementary materials.

2.1.1. Frequency estimation. For each integer value of the SNR (from 0 to 60 dB), we selected the signals corresponding to this SNR and plotted the average (left) and standard deviation (right) values of the corresponding errors in estimating the frequency (figure 4). The average indicates if there is a bias in measuring the frequency by this method while the standard deviation indicates the precision of the measure when there is no bias.

We clearly see, in the figure 4 (left), that all methods give good results when the SNR is high (greater than 40 dB). However, all methods but the Gabor fitting are biaised when SNR is low, with an average of overestimation of 10 to 30 % for SNR lower than 10 dB. An interesting case is the case of the centroid frequency. The value for this parameter is an average between the centroid frequency of the signal and the centroid frequency of the noise. As we used a gaussian noise of centroid frequency around 178 kHz (after high pass filtering at 100 kHz) and as the Gabor frequency of the synthetic clicks is on average 125 kHz, the centroid frequency has, in this case, a bias toward higher values. In the supplementary materials we show the case where signals have an average frequency of 190 kHz : the bias is then negative. This is quite important, since it means that, for a noisy signal, the centroid frequency measurement depends on the frequency window on which it is computed, and thus both on the instrument (such as the sample frequency f_s, usually varying from 384 kHz in modern Soundtraps to 576 kHz in the ST 300, which means a maximum frequency of $f_s/2$ in the spectrum) and on the post processing methods (high pass filtering at 100 kHz for instance). As a consequence, it is very delicate to compare centroid frequency between different experiments. The "sign change" method is also biased when the SNR is less than 12 dB. The fitting of a Gabor wavelet is also sensitive to noise, although it is not biased : when the SNR is less than 5 dB, the convergence of the fitting is

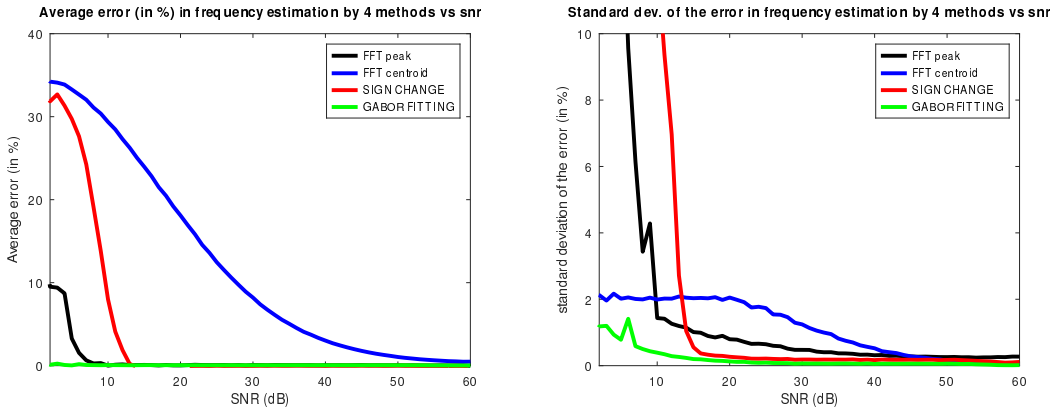

Figure 4 – Left : Average of errors (in %) on the estimation of the parameter f_0 as a function of signal to noise (in dB) for the 40000 synthesized Gabor wavelet clicks with added noise (see section 1.4). In black, estimation of f_0 by peak frequency measurement f_p (i.e. maximum of the spectrum). In blue, estimation of f_0 by centroid frequency f_c (i.e. the weighed mean frequency of the spectrum). In red, the estimation of f_0 by sign changes of the temporal signal. In green, the estimation of the frequency f_0 by the fitting of a Gabor wavelet. Right : Standard deviation of the errors (in %) on estimating parameter f_0 as a function of signal to noise (in dB) for the 40000 synthesized Gabor wavelet clicks (see section 1.4)

not good. When SNR is higher or equal to 5 dB, though, the convergence is achieved in more than 80% of the case (99% of the cases when SNR is higher than 8 dB). The peak frequency and fitting of a Gabor wavelet gives the best results and are non biaised methods. In general, for all methods, the precision is degraded when the SNR is below a defined threshold so we recommend to select only clicks with a SNR above this threshold for parameter estimation. In our case, only clicks with a SNR higher than 10 dB were selected for analysis in the following sections.

In the case of a distorted Gabor wavelet (see section 1.4), the results are quite similar (see supplementary materials). In the case of a Gabor wavelet with a replica, the results are similar concerning the average error. The estimation of the frequency is usually less precise, in accordance to section 1.3.4 (see figure 5 and supplementary materials). In this case, the precision of Gabor wavelet fitting is around 1% in average, better than peak frequency estimation (error of 2% in average, in coherence with figure 3, right). Thus, as replicas of the signal are quite common in the field recordings, it seems difficult to achieve a precision less than 1% in the measurements of the frequency of the NBHF clicks.

2.1.2. Duration and bandwidth estimation . For each integer value of the SNR (from 0 to 60 dB), we selected the signals corresponding to this SNR and average (left) and standard deviation (right) values of the corresponding errors in estimating the duration were computed (figure 6).

It is clear that, regardless of the method, the click duration is more difficult to measure than the frequency. The estimation of the duration T by Gabor fitting usually is not biased (fig. 6, left) when the SNR is above 5 dB. The other duration estimations are usually biased and the duration 'rms' seems very sensitive to noise and generally gives poor results as soon as the SNR is lower than 40 dB. Thus, this method of estimation of the duration of NBHF clicks has to be avoided. The precision in the estimation of the parameter T seems again better by fitting a Gabor wavelet, especially in a noisy context (fig. 6, right), however, no method reached a precision better

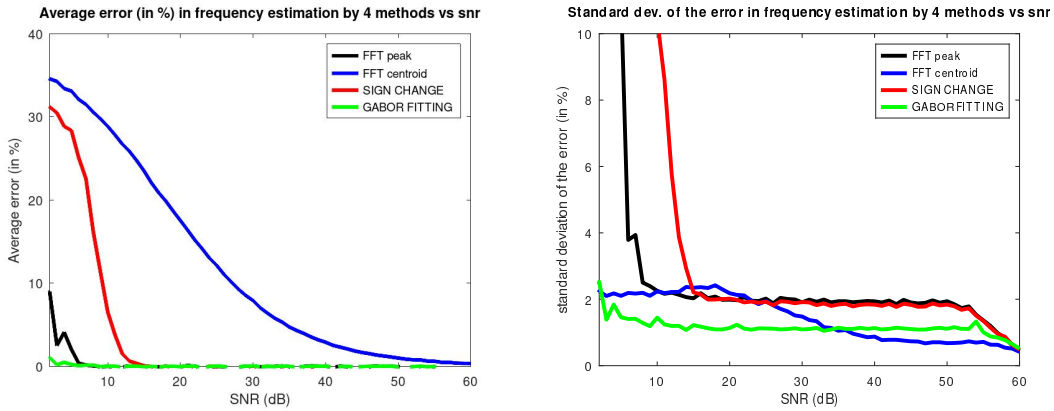

Figure 5 – Left : Average of errors (in %) on the estimation of the parameter f_0 as a function of signal to noise (in dB) for the 40000 synthesized Gabor wavelet clicks with a strong replica (see section 1.4). In black, estimation of f_0 by peak frequency measurement f_p (i.e. maximum of the spectrum). In blue, estimation of f_0 by centroid frequency f_c (i.e. the weighed mean frequency of the spectrum). In red, the estimation of f_0 by sign changes of the temporal signal. In green, the estimation of the frequency f_0 by the fitting of a Gabor wavelet. Right : Standard deviation of the errors (in %) on estimating parameter f_0 as a function of signal to noise (in dB) for the 40000 synthesized Gabor wavelet clicks (see section 1.4)

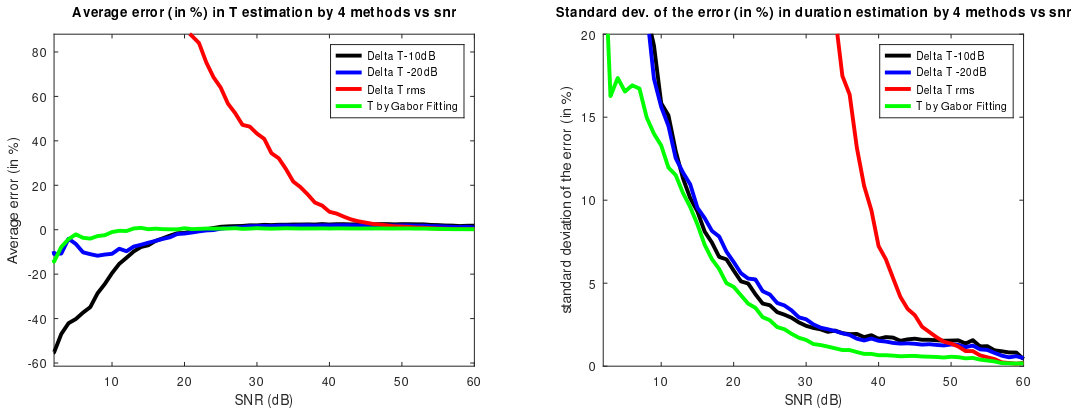

Figure 6 – Average (left) and standard deviation (right) of the percentage of error on the estimation of the duration parameters according to the signal to noise (in dB) by the four methods presented in section 1.4 : Δt_{-10dB}, Δt_{-20dB}, Δt_{rms} or Gabor fitting. The real value of each parameter is obtained by means of formulas of the table 1.

than 15 % for SNR lower than 10 to 15 dB. Estimation for distorted Gabor wavelet and Gabor wavelet with replica are presented in supplementary materials. For a distorted Gabor wavelet, all estimators tend to slightly underestimate the value of the duration which is coherent with an attenuation of the beginning of the wavelet by the distortion. In the presence of a replica these indicators are strongly degraded, as the duration of the signal is difficult to estimate (see section 1.3.4) but the Gabor wavelet fitting also gives the best results (precision of 10 to 30%, when the replica is not so strong, see supplementary materials). Concerning the estimation of T by means of bandwidth calculations, the classical methods to estimate frequency bandwidth present a bias for almost all SNR and could be discarded for the study of these signals (see figure 7). In particular, the estimations of $\Delta f_{-3\text{dB}}$ or $\Delta f_{-10\text{dB}}$ are not precise as the error in measuring these values is around 1 kHz while the actual values are of the order of 10kHz.

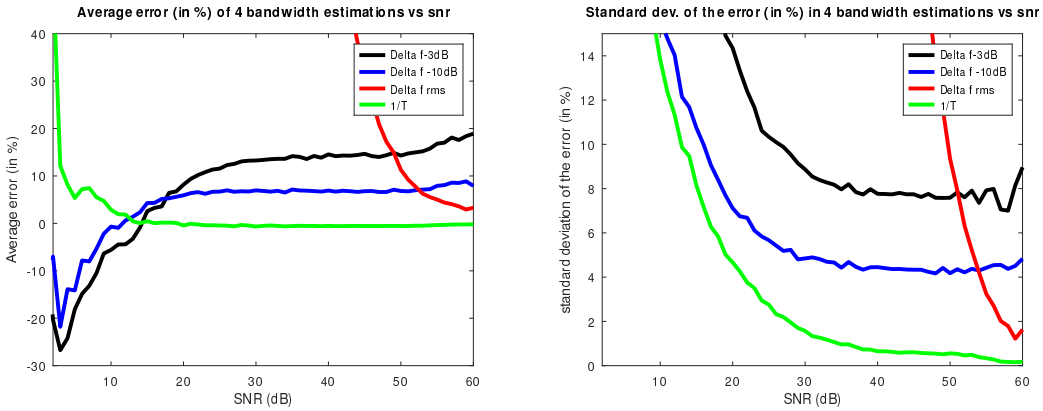

Figure 7 – Average (left) and standard deviation (right) of the percentage of error on the estimation of the bandwidths $\Delta f_{-10\text{dB}}$, $\Delta f_{-20\text{dB}}$, Δf_{rms} and bandwidth estimated by T_{Gabor} (see table 1) according to the signal to noise (in dB). The real value of each parameter is obtained by means of formulas of the table 1.

Taking into account these results we analyzed only clicks with a SNR above 10 dB in the data set of real clicks from Chaihuin and San Clemente del Tuyu and we computed only the frequencies estimations and the duration estimations.

2.2. Recordings, clicks detections and visual surveys

2.2.1. Acoustic and visual monitoring in Chaihuin, september 2023. During the four days of visual monitoring (33 hours of visual effort) only Peale's dolphins were seen in the Chaihuin bay. These moments of visual confirmation of the species correspond to 85 % of all clicks detected in the data set. No other NBHF species has been seen in the bay during September for several years (E. Montti personal communication). Therefore, we are rather confident that the NBHF clicks recorded during the experiment are from Peale's dolphins. The clicks from all instruments were first manually checked, and then only those with a SNR greater than 10 dB and with convergence of the Gabor fitting were selected (table 2).

Table 2 – *Number of clicks for each recording device (HighBlue channel 1, channel 2 and Soundtrap) at each step of the detections and selection process for the Chaihuin dataset. First line : all detections from the Octave routine. Second line : detections after manual revision. Third line : detections after manual revision with a SNR above 10 dB. Fourth line : detections after manual revision with a SNR above 10 dB and for which the fitting of a Gabor wavelet converged*

.

	HighBlue channel 1	HighBlue channel 2	Soundtrap
Detections	7743	8024	11718
Detections manually confirmed	6681	6580	9909
SNR $>$ 10dB	6537	6456	9529
SNR $>$ 10dB and convergence of the Gabor fitting	5243	4615	8052

To better compare the detections, we counted, for the two devices, only manually confirmed clicks in the 9 minutes chunks corresponding to the HighBlue files (N=6681 for HighBlue channel 1 / N=6580 for HighBlue channel 2 / N=9232 for Soundtrap) (fig. 8).

Both devices mostly agree on the moments where clicks are detected, as presented in other studies (Malige et al., 2025; Patris et al., 2023). Nine files were lost for the HighBlue device,

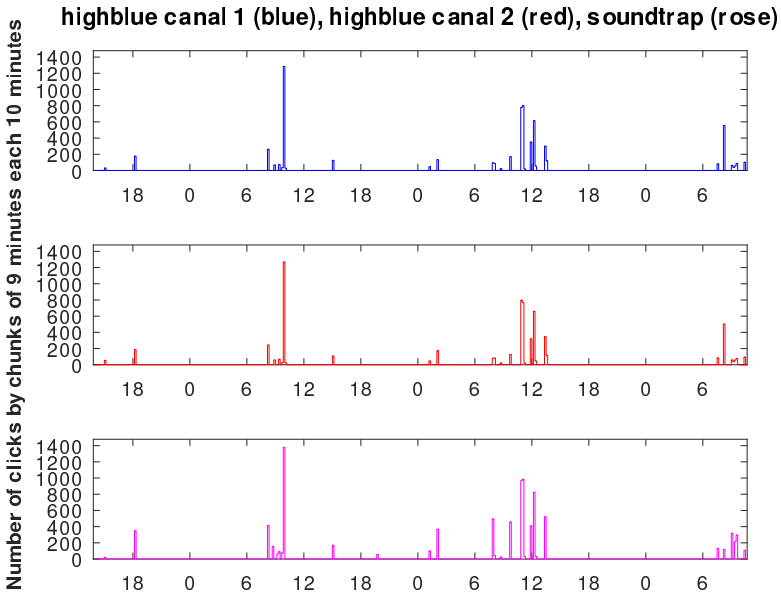

Figure 8 – Chaihuin dataset. Number of manually confirmed detections of clicks by chunks of 9 minutes in the HighBlue's files (canal 1 in blue and canal 2 in red) and soundtrap's files (in pink). The time is in local time and goes from the 21st of September until the 24th.

illustrating some failures of this device, which was still in development by SMIoT from Toulon university at the time of the experiment. Most of the clicks were detected in the morning, which is consistent with the visual survey : each day, various groups of Peale's dolphins of less than ten individuals entered the bay by the south between 8 am and 1 pm (local time). Their behavior was usually slow traveling toward the beach of the Chaihuin bay where they spent most of the day. There is a significant difference in the number of clicks recorded for each device. This difference could be due to the position and / or of the sensitivity of the recording devices. The self noise of the Soundtrap device is much lower than the self noise of the HighBlue device : the clicks have generally a better SNR for the Soundtrap (see figure 10 in supplementary materials). Sound files containing signals of Peale's dolphins are available at *https://zenodo.org/records/18019712*.

2.2.2. Acoustic and visual monitoring in San Clemente del Tuyu, september 2025. During the six days of acoustic monitoring, three visual surveys of 4h each were done, by boat, in the zone between the instruments and Punta Rasa (North of San Clemente del Tuyu). Only Franciscanas were seen during these surveys. San Clemente del Tuyu is within the extension zone of Burmeister's porpoise (*Phocoena spinipinnis*), but the low depth (2-4 m) in a large zone (few km wide) makes it very unlikely to find them there, and they have never been seen near San Clemente del Tuyu. Therefore, we are rather confident that the NBHF clicks recorded during the experiment are from Franciscanas, which are resident and have a very short range of displacement in this zone (Wells et al., 2021). The F-POD measures of the angle of the instrument indicated that the iron structure fell and was in horizontal position several times during the experiment. However, this F-POD was set up to record in any position and clicks were registered irrespectively when the structure was up or down. The same processing was applied as in the Chaihuin dataset, and table 3 gives the number of clicks at each step of the selection. Sound files containing signals of Franciscana's dolphins are available at *https://zenodo.org/records/18026145*.

Table 3 – *Number of clicks in each device (HighBlue channel 1, channel 2 and Soundtrap) at each step of the detections and selection of the clicks for San Clemente data set. First line : all detections from the Octave routine. Second line : detections after manual revision. Third line : detections after manual revision with a SNR above 10 dB. Fourth line : detections after manual revision with a SNR above 10 dB and for which the fitting of a Gabor wavelet converged*

.

	HighBlue channel 1	HighBlue channel 2	Soundtrap
Detections	3101	3144	7337
Detections manually confirmed	3037	3047	5642
SNR $>$ 10 dB	2575	2619	4642
SNR $>$ 10 dB and convergence of the Gabor fitting	2215	2335	4202

2.3. Click parameters

In this section, we give the results of the measurements of acoustic parameters of the datasets from Chaihuin and San Clemente del Tuyu. Only clicks with a SNR above 10 dB and for which the Gabor wavelet fitting converge are analyzed in this section according to the results of numerical tests (section 2.1).

2.3.1. Frequencies. In figure 9, we give the histograms of the peak frequency f_p, centroid frequency f_c and the Gabor frequency f_0 for the three devices (HighBlue, channel 1, top, HighBlue, channel 2, center and Soundtrap, bottom). The histograms of the peak frequency are rather different for the three devices (included between the two HighBlue channels) for both datasets. The histogram for the Soundtrap device has two marked different peaks. This is consistent with the remarks of section 1.3.4 and with figure 3 where the histogram of peak frequencies can be strongly dependent on the presence of the replicas. Because of the different sensitivities and positions of each instrument, the presence and intensity of replicas are quite variable. Therefore, peak frequency does not seem to be a stable way of measuring the frequency of NBHF clicks. As for the centroid frequency, the measure of this parameter is very sensitive to the background noise (as seen in section 2.1) and to the setting of each instrument (frequency cut off) and therefore for each device the distributions and averages are distinct. On the contrary, the Gabor frequency f_{Gabor} present histograms that are more similar, and with a distribution with less dispersion, which is also coherent with the remarks of section 1.3.4 (see table 4).

Table 4 – *Mean, standard deviation (mean $\pm$ standard deviation) and mode of peak, centroid and Gabor frequencies for HighBlue channel 1, channel 2 and Soundtrap (only clicks with frequencies less than 150 kHz were taken for the computation of the mean and standard deviation, in coherence with the histograms presented in figure 9)*

Frequency	Peak frequency f_p	Centroid frequency f_c	Gabor frequency f_{Gabor}
Chaihuin dataset / Peale's dolphins			
H.Blue, c. 1	124 $\pm$ 5 kHz / mode = 123 kHz	141 $\pm$ 5 kHz / mode = 140 kHz	124 $\pm$ 4 kHz / mode = 125 kHz
H.Blue, c. 2	127 $\pm$ 6 kHz / mode = 128 kHz	142 $\pm$ 5 kHz / mode = 143 kHz	126 $\pm$ 5 kHz / mode = 126 kHz
Soundtrap	126 $\pm$ 6 kHz / mode = 127 kHz	135 $\pm$ 4 kHz / mode = 133 kHz	125 $\pm$ 4 kHz / mode = 126 kHz
San Clemente dataset / Franciscana dolphins			
H.Blue, c. 1	133 $\pm$ 4 kHz / mode = 134 kHz	155 $\pm$ 4 kHz / mode = 153 kHz	134 $\pm$ 2 kHz / mode = 135 kHz
H.Blue, c. 2	133 $\pm$ 3 kHz / mode = 135 kHz	154 $\pm$ 4 kHz / mode = 155 kHz	133 $\pm$ 2 kHz / mode = 134 kHz
Soundtrap	131 $\pm$ 4 kHz / mode = 134 kHz	154 $\pm$ 6 kHz / mode = 157 kHz	132 $\pm$ 2 kHz / mode = 132 kHz

The averages of centroid frequency are not stable between instruments for the Chaihuin dataset, probably because of the lower frequency cut off of the ST 600, which biases the centroid

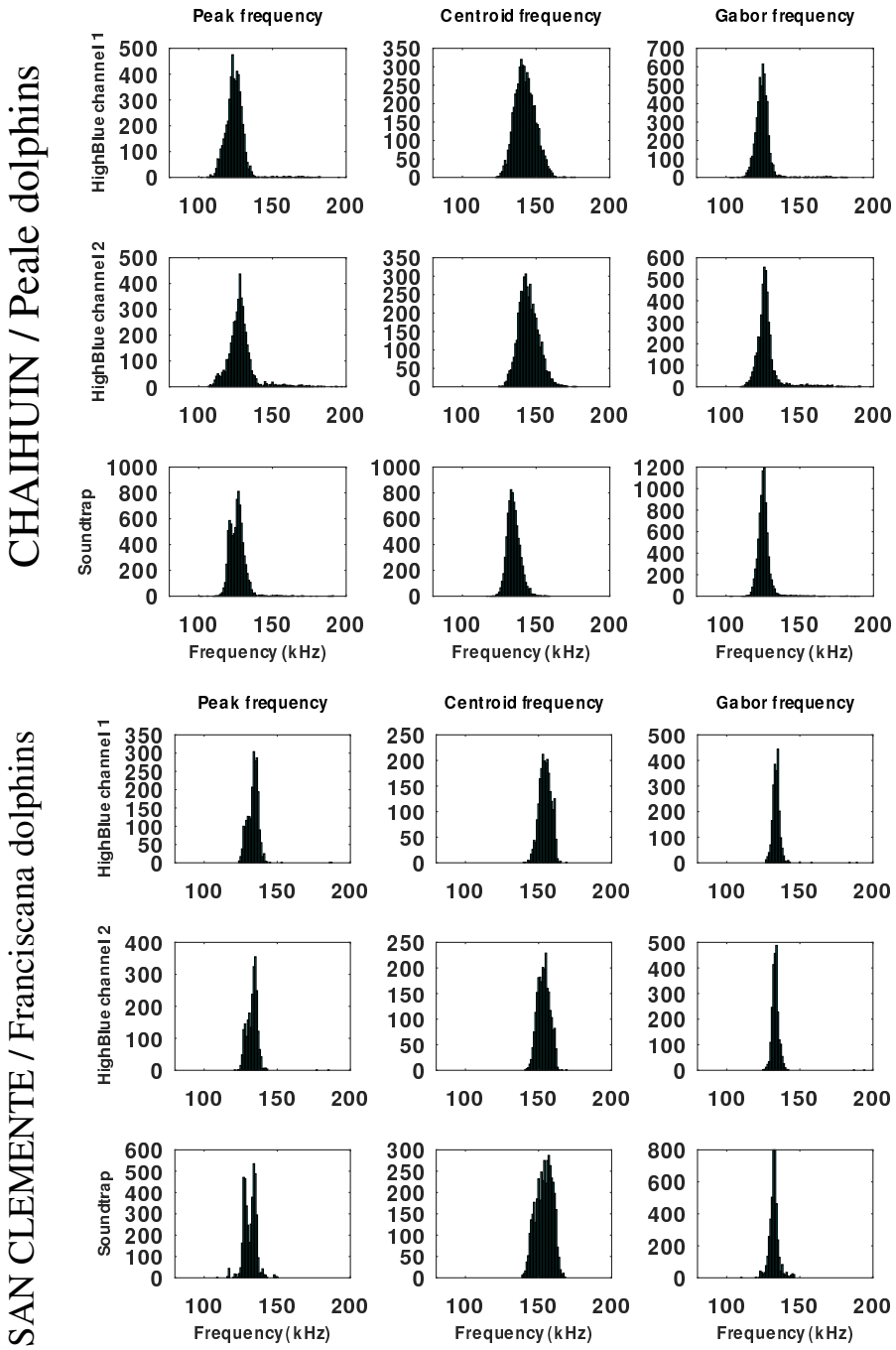

Figure 9 – *Top : Histograms of the frequency parameters for the two devices in* **Chaihuin** *dataset. Bottom : Histograms of the frequency parameters for the two devices in* **San Clemente del Tuyu** *data set. Only clicks for which the SNR is above 10 dB and the convergence of the Gabor wavelet fitting is achieved are selected. From top to bottom : HighBlue, channel 1, HighBlue, channel 2 and Soundtrap. from left to right : Peak frequency, centroid frequency, Gabor frequency.*

frequency towards low frequency (table 4). The values of the centroid frequency are on average much higher than the other frequency measures, which is coherent with the bias present when estimating this parameter (see supplementary materials and section 2.1, figure 4, left). As for peak frequency and Gabor frequency, the averages are rather stable between instruments and present a typical standard deviation around 5 kHz for the Chaihuin dataset, and around 3 kHz for

the San Clemente dataset, in both cases giving less dispersion for the Gabor frequency. The mode of the distribution is stable for the Gabor frequency and less stable for other measurements. There seems to be a robust difference between the frequencies of the two datasets, pointing towards a different signal from Franciscana and Peale's dolphin (see section 2.4).

2.3.2. Durations. Concerning the estimation of the duration of the signal, we give the histograms of $\Delta t_{-10\text{dB}}$, $\Delta t_{-20\text{dB}}$, Δt_{rms}, and Gabor duration T_{Gabor} for each dataset in the supplementary materials. Globally, the estimation of the duration by means of the Gabor duration is more stable than the other measures : the distributions of the durations are more stable between instruments for the Gabor duration (especially the modes and averages) (table 5). The dispersion of the data is similar for the measure of the durations except for the "rms" duration which is very sensitive to noise (see section 1.4) and has a very large dispersion.

Table 5 – *Mean, standard deviation (mean ± standard deviation) and mode (in μs) of $\Delta t_{-10\text{dB}}$, $\Delta t_{-20\text{dB}}$, Δt_{rms}, and Gabor duration T_{Gabor} for HighBlue channel 1, channel 2 and Soundtrap.*

Durations	$\Delta t_{-10\text{dB}}$	$\Delta t_{-20\text{dB}}$	Δt_{rms}	T_{Gabor}
Chaihuin dataset/ Peale's dolphins				
H.Blue, c. 1	81±28 / mode = 66	133±48 / mode = 106	120±70 / mode = 92	37±13 / mode = 32
H.Blue, c. 2	72±26 / mode = 68	122±45 / mode = 92	125±69 / mode = 46	34±14 / mode = 32
Soundtrap	81±26 / mode = 76	129±44 / mode = 102	96±50 / mode = 38	37±13 / mode = 32
San Clemente dataset / Franciscana dolphins				
H.Blue, c. 1	83± 23 / mode = 74	138 ± 41/ mode = 124	167 ± 69 / mode = 100	43 ± 11 / mode = 40
H.Blue, c. 2	85± 22 / mode = 74	139± 40 / mode = 118	149 ± 70 / mode = 72	43 ± 11 / mode = 42
Soundtrap	89 ± 22 / mode = 96	146 ± 46 / mode = 128	138± 45 / mode = 122	41 ± 11 / mode = 42

There is a strong link between the four computed durations for a Gabor wavelet (see table 1). To check this relation (and therefore to estimate the proximity of the dataset clicks and Gabor wavelet), for each selected click, we computed the ratio between Δt_{-10dB}, Δt_{-20dB}, Δt_{rms} and the value T_{Gabor}. These ratios are then compared with the theoretical value for a Gabor wavelet (see section 1.3.2). The ratios measured for the clicks of our data set are on average larger than the theoretical ratios (table 6). It could be due to the presence of replicas of the signal as seen in the section 1.3.4. Nevertheless, the ratios for Δt_{-10dB} are rather close to the theoretical values for a Gabor wavelet (table 1 and 6), and we can presume that the signals measured are then rather close to Gabor wavelets. The values in table 6 indicate that the parameter Δt_{-10dB} seems a bit less sensible to the replicas or to the noise than Δt_{-20dB} and clearly less than the "rms" duration Δt_{rms}. The fact that the measurement of $\frac{\Delta t_{rms}}{T_{\text{Gabor}}}$ is overestimated is mainly due to the fact that the computation of Δt_{rms} is biased toward higher values, including when the SNR is rather high (figure 6).

2.4. Comparison of the two datasets

2.4.1. Heat maps. A graphical comparison of the two datasets (fig. 10) was achieved by means of the use of the parameters f_{Gabor} and T_{Gabor} and, for comparison, with the parameters f_{peak} and $\Delta t_{-10\text{dB}}$, which are the most robust within the parameters classically used in other studies (see section 2.1). The heat maps presented in figure 10 show that the Gabor parameters give more focused heat maps and thus enable to better separate the two datasets.

Table 6 – *Mean and standard deviation (mean ± standard deviation) of the ratio of durations of the selected clicks and theoretical values for a Gabor wavelet (as presented in table 1)*

Ratio	$\frac{\Delta t_{-10dB}}{T_{\text{Gabor}}}$	$\frac{\Delta t_{-20dB}}{T_{\text{Gabor}}}$	$\frac{\Delta t_{rms}}{T_{\text{Gabor}}}$
Chaihuin dataset			
HighBlue, channel 1	2.25±0.55	3.85±1.63	3.64±2.73
HighBlue, channel 2	2.25±0.60	4.01±1.89	4.44±3.49
Soundtrap	2.29±0.56	3.86±1.67	2.94±2.05
San Clemente dataset			
HighBlue, channel 1	1.99±0.47	3.40±1.07	4.23±2.23
HighBlue, channel 2	1.99±0.44	3.30±0.95	3.71±2.16
Soundtrap	2.19±0.45	3.78±1.64	3.56±1.57
Theorical value for a Gabor wavelet	2.15	3.03	0.5

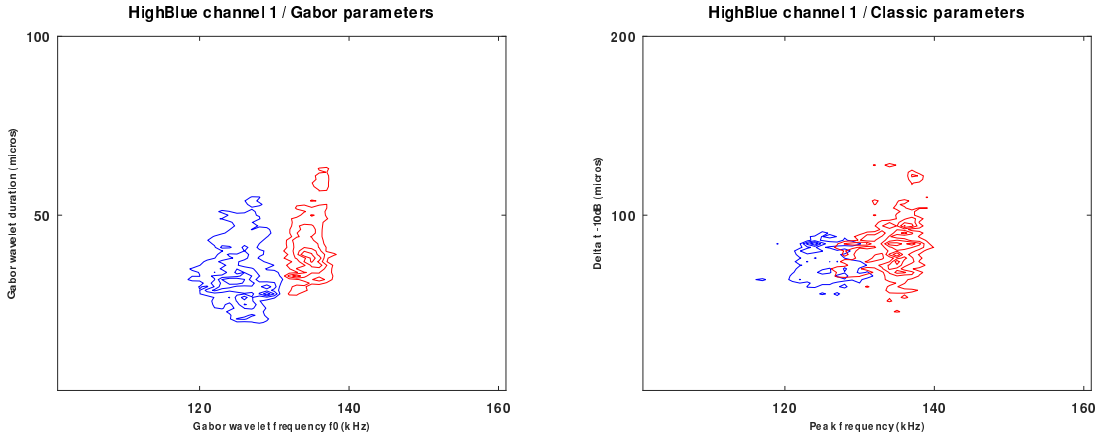

Figure 10 – *Heat maps of the clicks analyzed in HighBlue channel 1 (in each of the two figures, the Chaihuin dataset is represented in blue, and the San Clemente dataset in red). Left : heat map based on the Gabor frequency and duration (for each pixel of size 1 kHz/1μs, the normalized log of the number of clicks corresponding to this value is computed and a the contour of the density is plotted). Right : heat map based on the peak frequency and duration -10 dB (for each pixel of size 1kHz/2μs, the normalized log of the number of clicks corresponding to this value is computed and the contour of the density is plotted).*

2.4.2. Statistical analysis. The statistical analysis was centered on the four parameters (f_{Gabor}, f_{peak}, T_{Gabor} and $\Delta t_{-10\text{dB}}$). Considering the linear discriminant analysis, as expected for a two-group comparison, the analysis yielded a single discriminant axis, which separated the two species, with Peale's dolphins showing predominantly negative scores and Franciscana's dolphin positive scores. The discriminant function was dominated by the Gabor frequency (f_{gabor}; coefficient = 1.224), followed by the Gabor duration (T_{Gabor}; coefficient = 0.485), whereas the remaining parameters showed minor contributions. Cross-validated classification accuracy was approximately 85%, indicating a consistent multivariate separation between species. This analysis shows the importance of these two parameters (F_{gabor}, T_{Gabor}) to classify the clicks and their redundancy with f_{peak} and $\Delta t_{-10\text{dB}}$.

For the four parameters, the Wilcoxon rank-sum test gave extremely small p-values (smaller than 10^{-15}) when the two datasets were compared. It was expected as our datasets contain several thousands of clicks and significantly different average values. Therefore, we computed the p-value corresponding to the probability that a subset of 10 values (corresponding roughly

to the number of clicks in a click train) of a parameter coming from the San Clemente data set could belong to the Chaihuin data set, following the methodology proposed in Krzywinski and Altman, 2013. Accordingly to the figures 9 and the histograms for duration parameters in supplementary materials, we supposed that the statistical distribution of the parameters f_{Gabor}, f_{peak}, T_{Gabor} and $\Delta t_{-10\text{dB}}$ is normal. The values of the average and standard deviation were computed by the fitting of a Gaussian function (see supplementary materials). The p-values computed are extremely small for the frequency parameters f_{Gabor} and f_{peak} ($1\,10^{-12}, 3\,10^{-10}$). As for T_{Gabor} and $\Delta t_{-10\text{dB}}$, the p-value are 0.08 and 0.31 respectively. These values tend to indicate that the two species have very different frequency content and that it is possible to associate a train of clicks to one of these two species using the Gabor frequency estimation or the peak frequency. However, for the Gabor duration T_{Gabor} and $\Delta t_{-10\text{dB}}$, there is respectively 8% and 31% of chances of attributing clicks from the studied group of Franciscana to the group of studied Peale's dolphins using these parameters. This clear separation into very different frequencies and closer values in durations can be seen in heat maps from figure 10.

3. Conclusions

3.1. Mathematical study, numerical tests and comparison of the signal with Gabor wavelets

Analytical study and numerical tests are a good way to assess the eventual bias present in estimating acoustic parameters, as presented in section 2.1. Such an analysis, when it can be done, enables to better understand biological sounds. In our case, the use of a mathematical function (Gabor wavelet) as a model for NBHF clicks allows a clearer view of the interdependence of the parameters as well as their robustness considering the environment, the devices used and the replicas of the signal. Ratios in table 6, first column, indicate clearly that the echolocation clicks from Peale's dolphins or from Franciscana are globally close to Gabor wavelets.

A first conclusion of this study is that many classical acoustic parameters measured in various studies on NBHF clicks are redundant and that is is probably better to use few of them, well chosen and measured, in order to classify the clicks (by species or places for example). The fact that the five parameters of the Gabor wavelet (A,t_0,f_0,T,ϕ) are independent is of interest in the aim of classification. The parameters A and T are linked to the energy (table 1) and source level of a click. Thus the values of A and T have to be considered in propagation studies. We showed that Gabor frequency f_0 and duration T are stable parameters which are less impacted by the presence of replicas and could be used in future classification studies. The precise computation of values of t_0 could also help in studies of TDOA (time delay of arrival) when using an array to estimate the position of an animal. It is difficult to estimate the importance of the phase shift ϕ, which does not appear in most formulas of table 6 in the case of the polycyclic approximation. Nevertheless, the distribution of this parameter is coherent between devices in each dataset (see supplementary materials). It does not have a uniform repartition and the distribution is different in each data set. A more precise study of this parameter is still to be done and could be the purpose of future works.

Gabor wavelet is probably not the best mathematical model for other odontocetes emitting clicks with larger band and lower frequency as sperm whale or bottlenose dolphins. In this case, a set of other mathematical wavelets could be used, for example the "Mexican hat" function, best suited for oligocyclic signals (Ryan, 1994).

3.2. Species discrimination by acoustic parameters

The aim of our study was to assess several measures of acoustic parameters of the NBHF clicks and try to separate the dispersion coming from the data itself from the dispersion coming from the measurement method. By the use of synthesized signals and their analytical study we were able to estimate the error coming from the measurements. In the case of Gabor frequency measurement, this error is, for a good signal to noise ratio, less than 1% for a simple signal and about 2% for a signal with replica. This is the order of magnitude we find for field data in the case of the Franciscana, however, the dispersion of the data of the Peale's dolphin is about twice, which could be a signal that the Peale's dolphin emits less stereotyped NBHF signals, a conclusion consistent with the finding of other types of signals for Cephalorhynchus species (Martin et al., 2018, 2021; Martin et al., 2024) and not for the Franciscana.

A second conclusion of this study is that the frequency estimations present less uncertainty than duration and bandwidth estimations and are probably best suited to classify NBHF species (see results, section 2.1.2). Moreover, some acoustic parameters present some bias when estimated in a noisy context : centroid frequency and rms duration have to be avoided to measure the frequency and duration of these signals. The bandwidth measurements also present high uncertainty and are probably not the best tools to classify NBHF clicks.

The analysis done in this paper does not try to discriminate between on-axis or off-axis clicks as proposed in other studies (Götz et al., 2010; Kyhn et al., 2010). Such a distinction is difficult when the precise position of the emitter cannot be computed, all the more since coastal odontocetes like Franciscana are known to have a very mobile head. We simply decided to select only the high SNR clicks, considering that the animals, in the wild, are far enough so that a large part of the off-axis clicks (possibly attenuated by 20 dB or more, Macaulay et al., 2020), are probably lost.

The following step will be to use the Gabor frequency and Gabor duration parameters to try to separate between the six sympatric NBHF species that inhabit the South Cone of America : Peale's dolphin (*Cephalorhynchus australis*), Chilean dolphin (*Cephalorhynchus eutropia*), Commerson dolphin (*Cephalorhynchus commersonii*), Franciscana (*Pontoporia blainvillei*), Burmeister's porpoise (*Phocoena spinipinnis*) and spectacled porpoise (*Phocoena dioptrica*). This method (or a similar one with other mathematical models, more suited to the signal studied) could also be used to assess the acoustic separation of other species :

- between other sympatric NBHF species (harbor porpoise and Dall's porpoise in British Columbia, Kyhn et al., 2013),
- between similar species as pygmy and dwarf sperm whale (*Kogia breviceps* and *Kogia sima*) (Hildebrand et al., 2019),
- between Sotalia and Inia species in the Amazon river (Kamminga et al., 1993),
- between the Zyphius species, where the acoustic classification is still very incomplete (Cheung and O'Brien, 2025).

3.3. Summary /main conclusions

- The combination of analytical and numerical studies of mathematical functions enables to have a clearer view of the acoustic parameters of NBHF clicks and of the best way to measure them.

- Some classical acoustic parameters used to classify odontocetes are redundant and some have to be avoided because they are very sensitive to noise or propagation.
- Peale's and Franciscana dolphins from the two data sets studied emit different NBHF clicks. The main difference resides in the frequency content of the clicks.

Acknowledgements

We thank Fernanda Zapata and Claudio Silva (NGO AquaMarina, Argentina), as well as Felipe Araya Fernández (NGO Vuelve al Oceano, Chile) for their help in the field work. We thank Régine Guillermin and Paul Cristini from LMA laboratory of Aix-Marseilles university for their help in calibrating the HighBlue acquisition chain. Computation and figures of this report were done using OCTAVE (Eaton et al., 2009) or the R software (R Foundation for Statistical Computing, 2024). Audacity software was used for annotation of the files.

Fundings

We thank the SMIoT team in Toulon university (Valentin Barschasz, Valentin Gies, Sebastian Marzetti), who designed, built and loaned the HighBlue device. This study was done in the mark of the IRP project "Détection et Classification IA des Biosonars des dauphins et marsouins du Cône Sud" (DCBD), funded by CNRS (France).

Conflict of interest disclosure

The authors declare that they comply with the PCI rule of having no financial conflicts of interest in relation to the content of the article.

References

Acevedo J (2011). *Análisis y observación de delfines en canal Fitz Roy, Río Verde (Spanish)*. Tech. rep. Fundación CEQUA.

Amorim T, de Castro FR, Ferreira G, Neri F, Duque B, Mura J, Andriolo A (2022). Acoustic identification and classification of four dolphin species in the Brazilian marine area affected by the largest tailings dam failure disaster. *The Journal of the Acoustical Society of America* **152**, 3204–3215. https://doi.org/10.1121/10.0016358.

Amundin M, Carlström J, Thomas L, Carlén I, Koblitz J, Teilmann J, Tougaard J, Tregenza N, Wennerberg D, Loisa O, Brundiers K, Kosecka M, Kyhn L, Ljungqvist C, Sveegaard S, Burt M, Pawliczka I, Jussi I, Koza R, Benke H (2022). Estimating the abundance of the critically endangered Baltic Proper harbour porpoise (Phocoena phocoena) population using passive acoustic monitoring. *Ecology and Evolution* **12**. https://doi.org/10.1002/ece3.8554.

Andriolo A, Sucunza F, Zerbini A, Danilewicz D, Cremer M, Holz A (2014). Preliminary calculation of individual echolocation signal emission rate of Franciscana dolphins (Pontoporia blainvillei). *The Journal of the Acoustical Society of America* **136**, 2277–2277. https://doi.org/10.1121/1.4900228.

Au W, Kastelein R, Rippe T, Schooneman N (1999). Tranmission beam pattern and echolocation signals of a harbor porpoise (Phocoena phocoena). *The Journal of the Acoustical Society of America* **106**, 3699–705. https://doi.org/10.1121/1.428221.

Au W (1993). *The sonar of dolphin*. Springer.

Barchasz V, Gies V, Marzetti S, Glotin H (2020). A Novel Low-Power High Speed Accurate and Precise DAQ with Embedded Artificial Intelligence for Long Term Biodiversity Survey. In: *Proceedings of the Forum Acusticum*. Lyon, France.

Bastida R, Rodriguez D, Secchi E, DaSilva V (2022). *Mamíferos acuáticos de Sudamérica y Antártida. 2ª ed.* Ed. M. Vázquez y M. Mazzini. Ciudad Autónoma de Buenos Aires.

Cheung B, O'Brien J (2025). Exploring the Occurrences of Beaked Whales off the West Coast of Ireland Through Passive Acoustic Monitoring (PAM). *Journal of Marine Science and Engineering* **13**, 1618. https://doi.org/10.3390/jmse13091618.

Eaton JW, Bateman D, Hauberg S (2009). *GNU Octave version 3.0.1 manual: a high-level interactive language for numerical computations*. CreateSpace Independent Publishing Platform. URL: http://www.gnu.org/software/octave/doc/interpreter.

Fang L, Wang D, Li Y, Cheng Z, Pine M, Wang K, Li S (2015). The Source Parameters of Echolocation Clicks from Captive and Free-Ranging Yangtze Finless Porpoises (Neophocaena asiaeorientalis asiaeorientalis). *PLoS ONE* **10**, e0129143. https://doi.org/10.1371/journal.pone.0129143.

Finfer D, White P, Chua G, Leighton T (2012). Review of the occurrence of multiple pulse echolocation clicks in recordings from small odontocetes. *IET Radar Sonar Navigation* **6**.

Gabor D (1946). Theory of Communication. *Journal of the Institution of Electrical Engineers* **93**, 429–441.

Galatius A, Kinze C, Olsen M, Tougaard J, Gotzek D, McGowen M (2025). Phylogenomic, morphological and acoustic data support a revised taxonomy of the lissodelphinine dolphin subfamily. *Molecular Phylogenetics and Evolution* **205**, 108299. https://doi.org/10.1016/j.ympev.2025.108299.

Giardino G, Cosentino M, Macchi A, Loureiro J, Rodriguez S, Alvarez K, Moron S, Rodriguez D (2024). Detailed Comparison of Acoustic Signals from Rehabilitated and Wild Franciscanas (Pontoporia blainvillei) Dolphins. *Animals*.

Goold JC, Jones SE (1995). Time and frequency domain characteristics whale of sperm clicks. *Journal of Acoustic society of America*.

Götz T, Antunes R, Heinrich S (2010). Echolocation clicks of free-ranging Chilean dolphins (*Cephalorhynchus eutropia*). *The Journal of the Acoustical Society of America* **128**, 563–6.

Heinrich S, Genov T, Riquelme M, Hammond P (2019). Fine scale habitat partitioning of Chilean and Peale's dolphins and their overlap with aquaculture. *Aquatic Conservation: Marine and Freshwater Ecosystems* **29**, 212–226.

Hildebrand J, Frasier K, Baumann-Pickering S, Wiggins S, Merkens K, Garrison L, Soldevilla M, Mcdonald M (2019). Assessing Seasonality and Density From Passive Acoustic Monitoring of Signals Presumed to be From Pygmy and Dwarf Sperm Whales in the Gulf of Mexico. *Frontiers in Marine Science* **6**, 66. https://doi.org/10.3389/fmars.2019.00066.

Hucke-Gaete R, Bedriñana-Romano L, Viddi F, Acevedo J, Buchan S, Sielfeld W, Aguayo-Lobo A, Cari I, Zerbini A, Zarate P, Valencia J, Collao D (2024). *Diseño para la estimación poblacional de cetáceos en aguas jurisdiccionales de Chile*. Tech. rep. Centro Ballena Azul, Subpesca.

Jaramillo Legorreta AM, Cardenas Hinojosa G, Nieto E, Rojas-Bracho L, Thomas L, Ver Hoef J, Moore J, Taylor B, Barlow J, Tregenza N (2019). Decline towards extinction of Mexico's vaquita porpoise (Phocoena sinus). *Royal Society Open Science* **6**, 190598.

Kamminga C, Cohen-Stuart A, Silber G (1996). Investigations on cetacean sonar XI : Intrinsic comparison of the wave shapes of some members of the phocoenidae family. *Aquatic mammals* **22**, 45–55.

Kamminga C, Kataoka T, Engelsma F (1986). Investigations on cetacean sonar VII : Underwater sounds of Neophocaena phocaenoides of the Japanese coastal population. *Aquatic mammals* **12**, 52–60.

Kamminga C, VanHove M, Engelsma F, Terry R (1993). Investigations on cetacean sonar X : a comparative analysis of underwater echolocation clicks of Inia spp. and Sotalia spp. *Aquatic mammals* **19**, 31–43.

Kimura S, Akamatsu T, Li S, Dong S, Dong L, Wang K, Wang D, Arai N (2010). Density estimation of Yangtze finless porpoises using passive acoustic sensors and automated click train detection. *J. Acoust. Soc. Am.* **128**, 1435–1445.

Krzywinski K, Altman N (2013). Significance, P values and t-tests. *Nature*, 809–810.

Kyhn L, Tougaard J, Beedholm K, Jensen F, Ashe E, Williams R, Madsen P (2013). Clicking in a Killer Whale Habitat: Narrow-Band, High-Frequency Biosonar Clicks of Harbour Porpoise (Phocoena phocoena) and Dall' s Porpoise (Phocoenoides dalli). *PloS one* **8**, e63763. https://doi.org/10.1371/journal.pone.0063763.

Kyhn L, Tougaard J, Jensen F, Wahlberg M, Stone G, Yoshinaga A, Beedholm K, Madsen P (2009). Feeding at a high pitch: Source parameters of narrow band, high-frequency clicks from echolocating off-shore hourglass dolphins and coastal Hector's dolphins. *The Journal of the Acoustical Society of America* **125**, 1783–91. https://doi.org/10.1121/1.3075600.

Kyhn L, Jensen F, Beedholm K, Tougaard J, Hansen M, Madsen P (2010). Echolocation in sympatric Peale's dolphins (Lagenorhynchus australis) and Commerson's dolphins (Cephalorhynchus commersonii) producing narrow-band high-frequency clicks. *The Journal of experimental biology* **213**, 1940–9.

Lelandais F, Glotin H (2008). Mallat's Matching Pursuit of sperm whale clicks in real-time using Daubechies 15 wavelets. In: *2008 New Trends for Environmental Monitoring Using Passive Systems*, pp. 1–5. https://doi.org/10.1109/PASSIVE.2008.4786977.

Li S, Wang K, Wang D, Akamatsu T (2005). Echolocation signals of the free-ranging Yangtze finless porpoise (Neophocaena phocaenoides asiaorientialis). *The Journal of the Acoustical Society of America* **117**, 3288–96. https://doi.org/10.1121/1.1882945.

Macaulay J, Malinka C, Gillespie D, Madsen P (2020). High resolution three-dimensional beam radiation pattern of harbour porpoise clicks with implications for passive acoustic monitoring. *The Journal of the Acoustical Society of America* **147**, 4175–4188.

Madhusudhana S, Gavrilov A, Erbe C (2015). Automatic detection of echolocation clicks based on a Gabor model of their waveform. *The Journal of the Acoustical Society of America* **137**, 3077–3086. https://doi.org/10.1121/1.4921609.

Malige F, Patris J, Caceres B, Poblete J, Glotin H, Saravía M, C.Alarcon-Vera, Barchasz V, Gies V, S. Marzetti MFR, Filún D (2025). Acoustic and visual monitoring of Peale's Dolphins (Lagenorhynchus australis) in the Magellan strait. *PeerJ*.

Malige F, Patris J, Silvestri M, Pereira R, Aguilar A, Soto M, Molina V, Hinojosa I, Sotomayor F, Calderón C, Montti E, Caceres B, Poblete J, Saravía M, Filún D, Glotin H (2024). Tools for the classification of NBHF species in Southern Chile. Poster in the international conference DCLDE in Rotterdam.

Malinka C, Tonnesen P, Dunn C, Claridge D, Gridley T, Elwen S, Madsen P (2021). Echolocation click parameters and biosonar behaviour of the dwarf sperm whale (Kogia sima). *Journal of Experimental Biology* **224**, jeb240689. https://doi.org/10.1242/jeb.240689.

Marques TA, Thomas L, Martin SW, Mellinger DK, Ward JA, Moretti DJ, Harris D, Tyack PL (2013). Estimating animal population density using passive acoustics. *Biol. Rev.* **88**, 287–309.

Martin M, Elwen S, Kassanjee R, Gridley T (2019). To buzz or burst-pulse? The functional role of Heaviside's dolphin, Cephalorhynchus heavisidii, rapidly pulsed signals. *Animal Behaviour* **150**.

Martin M, Gridley T, Elwen S, Jensen F (2018). Heaviside's dolphins (Cephalorhynchus heavisidii) relax acoustic crypsis to increase communication range. *Proceedings of the Royal Society B: Biological Sciences* **285**.

Martin M, Torres Ortiz S, Reyes Reyes M, Marino A, Iniguez M, Wahlberg M (2021). Commerson's dolphins (Cephalorhynchus commersonii) can relax acoustic crypsis. *Behavioral Ecology and Sociobiology* **75**. https://doi.org/10.1007/s00265-021-03035-y.

Martin MJ, Torres Ortiz S, Wahlberg M, Weir CR (2024). Peale's dolphins (Laghenorhynchus australis) are acoustic mergers between dolphins and porpoises. *Journal of Experimental Marine Biology and Ecology* **572**. https://doi.org/10.1016/j.jembe.2023.151977.

Melcon M, Failla M, Iniguez M (2016). owards Understanding the Ontogeny of Echolocation in Franciscana Dolphins (Pontoporia blainvillei). *Marine Mammal Science* **32 (4)**, 1516–1521.

Merkens K, Mann D, Janik V, Claridge D, Hill M, Oleson E (2018). Clicks of dwarf sperm whales (Kogia sima). *Marine Mammal Science* **34**. https://doi.org/10.1111/mms.12488.

Morgenthaler A, Fernández J, Moraga R, Olavarria C (2014). Chilean dolphins on the Argentine Atlantic coast. *Marine Mammal Science* **30**. https://doi.org/10.1111/mms.12052.

Morisaka T, Karczmarski L, Akamatsu T, Sakai M, Dawson S, Thornton M (2011). Echolocation signals of Heaviside' s dolphins (Cephalorhynchus heavisidii). *The Journal of the Acoustical Society of America* **129**, 449–57. https://doi.org/10.1121/1.3519401.

Nielsen N, Dawson S, Torres Ortiz S, Wahlberg M, Martin M (2024). Hector's dolphins (Cephalorhynchus hectori) produce both narrowband high-frequency and broadband acoustic signals. *The Journal of the Acoustical Society of America* **155**, 1437–1450. https://doi.org/10.1121/10.0024820.

Paitach R, Bortolotto G, Amundin M, Cremer M (2023). Critically endangered franciscana dolphins in an estuarine area: fine-scale habitat use and distribution from acoustic monitoring in Babitonga Bay, southern Brazil. *Marine Ecology Progress Series* **707**. https://doi.org/10.3354/meps14249.

Patris J, Malige F, Hamame M, Glotin H, Barchasz V, Gies V, Marzetti S, Buchan S (2023). Medium-term acoustic monitoring of Patagonian coastal dolphins. *PeerJ*.

R Foundation for Statistical Computing A (Vienna) (2024). R: A language and environment for statistical computing.

Reyes Reyes M, Iniguez M, Hevia M, Hildebrand J, Melcon M (2015). Description and clustering of echolocation signals of Commerson's dolphins (Cephalorhynchus commersonii) in Bahia San Julian, Argentina. *The Journal of the Acoustical Society of America* **138**, 2046.

Reyes Reyes V, Marino A, Dellabianca N, Hevia M, Torres M, Raya Rey A, Melcón M (2018). Clicks of wild Burmeister's porpoises (Phocoena spinipinnis) in Tierra del Fuego, Argentina: NOTES. *Marine Mammal Science* **34**.

Ryan H (1994). Ricker, Ormsby, Klauder, Butterworth : A Choice of wavelets. *CSEG recorder*.

Silva D, Barbosa R, Conversani V, Botta S, Hohn A, Santos M (2020). Reproductive parameters of franciscana dolphins (Pontoporia blainvillei) of Southeastern Brazil. *Marine Mammal Science* **36**.

Soldevilla M, Henderson E, Campbell G, Wiggins S, Hildebrand J, Roch M (2008). Classification of Risso's and Pacific white-sided dolphins using spectral properties of echolocation clicks. *The Journal of the Acoustical Society of America* **124**, 609–24. https://doi.org/10.1121/1.2932059.

Soldevilla M, Wiggins S, Hildebrand J (2010). Spatial and temporal patterns of Risso's dolphin echolocation in the Southern California Bight. *The Journal of the Acoustical Society of America* **127**, 124–32. https://doi.org/10.1121/1.3257586.

Song Z, Zhang Y, Wang X, Wei C, Wu F, Miao X (2017). Vocalizations of a wild finless porpoise (Neophocaena asiaeorientalis sunmeri) in the western coast of the Taiwan Strait, China. *Journal of Biobased Materials and Bioenergy* **11**, 45–52. https://doi.org/10.1166/jbmb.2017.1642.

Tougaard J, Kyhn L (2009). Echolocation sounds of hourglass dolphins (Lagenorhynchus cruciger) are similar to the narrow band high frequency echolocation sounds of the dolphin genus Cephalorhynchus. *Marine Mammal Science* **26**, 239–245. https://doi.org/10.1111/j.1748-7692.2009.00307.x.

Tregenza N (2014). *CPOD.exe: a guide for users*. Tech. rep. Chelonia Ltd.

Trone M, Glotin H, Balestriero R, Bonnett D, Blakefield J (2015). Heterogeneity of Amazon River dolphin high-frequency clicks: Current Odontoceti bioacoustic terminology in need of standardization. *Proceedings of Meetings on Acoustics* **22**. https://doi.org/10.1121/2.0000028.

Venables W, Ripley B (2002). Modern Applied Statistics with S, Fourth Edition. In: ed. by New York Springer.

Verluis M, von der Heydt A, Lohse D, Schmitz B (2000). How Snapping Shrimp Snap : Through Cavitating Bubbles. *Science*.

Villadsgaard A, Wahlberg M, Tougaard J (2007). Echolocation signals of wild harbour porpoises, Phocoena phocoena. *The Journal of experimental biology* **210**, 56–64. https://doi.org/10.1242/jeb.02618.

Wells R, Cremer M, Berninsone L, Albareda D, Wilkinson K, Stamper M, Paitach R, Bordino P (2021). Tagging, ranging patterns, and behavior of franciscana dolphins (Pontoporia blainvillei) off Argentina and Brazil: Considerations for conservation. *Marine Mammal Science* **38**. https://doi.org/10.1111/mms.12879.

Wiersma H (1982). Investigation on cetacean sonar IV : A comparison of wave shapes of odontocetes sonar signals. *Aquatic mammals* **9**.

Zimmer WMX (2011). *Passive Acoustic Monitoring of Cetaceans*. Cambridge University Press.